Fig. 2: Both the Bragg grommetry and small q range detection systems are centered to the sample.

References

A. Sakdinawat, and D. Attwood, Nat. Photonics **4**, 840 (2010).

J. Miao, P. Charalambous, J. Kirz, and D. Sayre, Nature **400**, 342 (1999).

I. K. Robinson, I. A. Vartanyants, G. J. Williams, M. A. Pfeifer, and J. A. Pitney, Phys. Rev. Lett. **87**, 195505 (2001).

J. Miao, T. Ishikawa, B. Johnson, E. H. Anderson, B. Lai, and K. O. Hodgson, Phys. Rev. Lett. **89**, 088303 (2002).

J. M. Rodenburg, and H. M. L. Faulkner, Appl. Phys. Lett. **85**, 4795 (2004).

M. C. Newton, S. J. Leake, R. Harder, and I. K. Robinson, Nat. Mater. **9**, 120 (2010).

A Projection and Transmission X-ray Microscope

X-ray imaging was the first application of X-rays one hundred years ago. With a third-generation synchrotron source, the X-ray imaging capability is greatly improved through advanced techniques of acquisition, detection and data analysis.

High-resolution X-ray imaging (direct) is currently able to attain a spatial resolution 30 nm or less.[1-3] For high-speed X-ray imaging, the temporal resolution can be as great as several tens of microseconds;[4] the resolution in tomography can be as great as 10 Hz.[5,6] For a projection microscope, the phase contrast can be obtained with a grating interferometer[7] or be propagation-based,[8,9] and a method with one single shot has been proposed.[10] In a transmission X-ray microscope, the general approach to obtain the phase contrast is Zernike's phase contrast,[11] and is propagation-based.[12]

For a material analysis, an X-ray absorption spectrum (XAS) is a widely used method involving scanning the energy near the absorption edge of a specific element. A Si(111) double-crystal monochromator provides high resolution, whereas a multi-layer monochromator is applied for an application with greater flux.

A transmission X-ray microscope (TXM) was installed in **TLS 01B** in 2004. Its greatest optical resolution is better than 30 nm in 2D (third order) and better than 60 nm (first order), and is near 60 nm in 3D.[2] This microscope is equipped for phase contrast with both Zernike phase contrast and propagation-based.[12] This instrument was the first TXM to use a capillary as a condenser; this design provides about ten times the intensity of the traditional type that uses a zone plate as a condenser. After that development in NSRRC, SSRL, APS, BNL and many other facilities adopted this concept to produce a new type of TXM. As this TXM was the first of this new type, some functions were not considered at the time that it was built, such as a capability to record an X-ray absorption spectrum (XAS). As that old type of TXM limited the sample size to about 15 mm, we plan to build a new endstation that accommodates a projection X-ray microscope (PXM) and a TXM at the same beamline.

The PXM provides a direct image, which means that no optical component intervenes between the source, sample and detector. The source can be a parallel beam or a focused beam. In our new setup for **TPS 31A**, we use a parallel beam in order to maximize the photon energy and flux.

Beamline Design

TPS 31A wiggler W100 is chosen for the PXM and TXM beamline, because its flux is about 100 times as great as that from a bending magnet at photon energy 50 keV. The PXM beamline is designed for energy range 5–50 keV. The brilliance is 4.9×10^{17} to 5.8×10^{16} photons s^{-1} $mrad^{-2}$ mm^{-2} per 0.1 % BW per 0.5A; the photon flux is 2.6×10^{14} to 8.9×10^{12} photons s^{-1} $mrad^{-1}$ per 0.1 % BW per $0.5A^{-1}$ for energy range 5–50 keV.

The optical layout of the **TPS 31A** PXM/TXM beamline is shown in **Fig. 1**. Endstation PXM (ES PXM) is designed for a projection microscope (PXM) and a transmission X-ray microscope TXM (ES TXM). The fan of horizontal radiation of this beamline is 1.5 mrad. After the front-end section located inside the radiation-shielding wall, the photon beam becomes defined with a water-cooled aperture and passes through a Be filter (thickness 600 μm), which removes low-energy photons and decreases the radiant power. One Be window (thickness 250 μm) is located between the Be filter chamber and the DCM chamber to protect the UHV upstream of the DCM. The other Be window (thickness 250 μm) is located at the end of the beamline chamber to separate the UHV section from the endstation at atmospheric pressure.

This beamline is designed with four operating modes, described as follows. (1) In a PXM with white light mode, the layout is shown as in **Fig. 1(a)**. In addition to the optical components mentioned above, we added a two-slit system to define the beam size and to monitor the beam position. (2) In a PXM with double-multilayer monochromator (DMM) mode, the layout is illustrated as in **Fig. 1(b)**. A DCM/DMM, with double Si(111) crystals and double Mo-B_4C/Si multilayers cooled with liquid nitrogen, is located 29 m from the source. Operating in the DMM mode, we adopt double Mo-B_4C/Si multilayers to select a monochromatized beam with energy resolution about 1% over energy range 5–30 keV. (3) In a PXM with double-crystal monochromator (DCM) mode (**Fig. 1(c)**), a tangential cylindrical vertical collimating mirror (VCM) with water cooling is located 25 m from the source to form a parallel beam for a double-crystal monochromator (DCM). Operating in the PXM DCM mode, we chose double Si(111) crystals to select the monochromatized beam with energy resolution = 1.37×10^{-4} to 2.5×10^{-4} over energy range 5–30 keV. (4) In a TXM with a double-crystal monochromator (DCM) mode (**Fig. 1(d)**), in addition to the VCM and DCM mentioned in (3) for the PXM with DCM mode, we added one horizontal focusing mirror (HFM) located 32 m and one vertical focusing mirror located 44.5 m for spatial resolution 30 nm as a transmission X-ray microscope (TXM). The flux of each mode is shown in **Fig 2**.

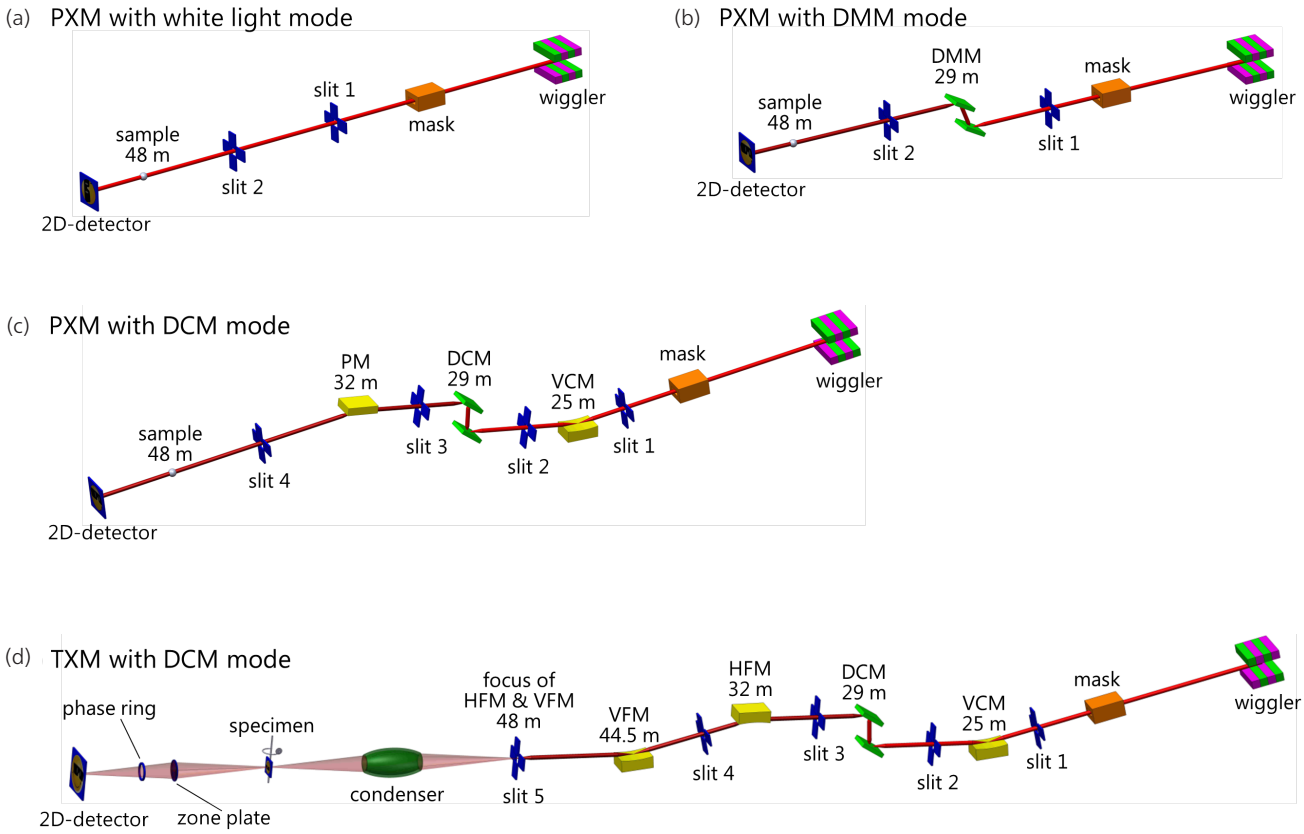

Fig. 1: Optical layout of the **TPS 31A** PXM/TXM beamline. (a) PXM in white-light mode; (b) PXM in double-multilayer monochromator (DMM) mode; (c) PXM in double-crystal monochromator (DCM) mode; (d) TXM in double-crystal monochromator (DCM) mode.

Design of the endstation

This endstation can be divided into three main parts – the projection X-ray microscope (PXM) module, the transmission X-ray microscope module and the detector module, as shown in **Fig. 3**.

(1) TXM module. This transmission X-ray microscope is based on a zone plate with a capillary as the condenser. The designed energy range is 5–12 keV according to the best optical efficiency of a zone plate. This microscope, designed with resolution better than 30 nm, has a working distance larger than 3 cm at energy 5 keV. The distance from the zone plate to the detector is from 1 m to 4.6 m. The structure of the TXM module is illustrated in **Fig. 4** below. The TXM consists of a stop, condenser, sample stage, zone-plate stage and a phase ring. A pinhole can be placed between the condenser and a sample stage if the direct beam is not completely blocked.

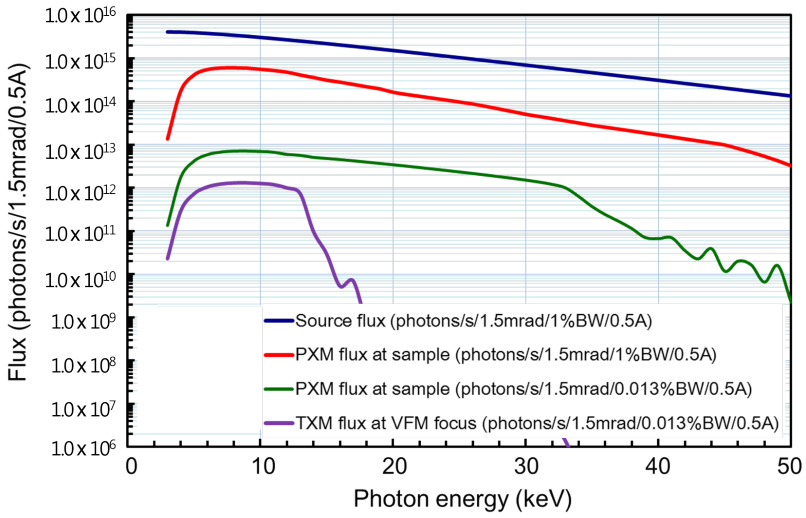

Fig. 2: Photon flux of the **TPS 31A** PXM/TXM beamline at the sample position

(2) In the projection X-ray microscope (PXM) module, this PXM is aimed for direct projection, with no optics in this module; the resolution depends mainly on the resolution of a scintillator, which is introduced in the detector module. The PXM module consists of a high-speed air-bearing rotation stage, and two linear stages. The rotation stage will have a three-axis positioner for adjustment of the sample position. A drawing of the conceptual design appears in **Fig. 5**.

(3) The detector module consists mainly of a three-axis stage, a high-speed area detector and optical objectives, which are for 5×, 10×, 20× and 100×. Its use is planned for both TXM and PXM modules. For TXM, a 20× objective serves for X-ray magnification about 50×, which is 1000× for a detector pixel size about 10 μm. The effective pixel size is about 10 nm, which provides sufficient over-sampling for a system of resolution 30 nm. For a PXM system, the optical objective can be from 100× for the greatest resolution, which is limited to about 0.5 μm by the scintillator, or another magnification can be selected for a large field of view (FOV). The structure of the detector module is depicted in **Fig. 6**.

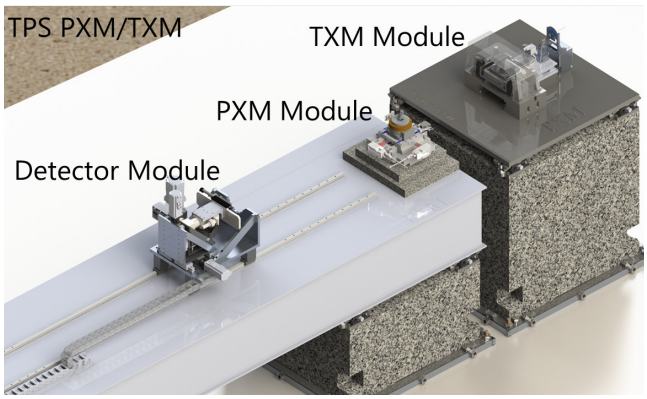

Fig. 3: TXM consisting of three main parts – TXM module, PXM module and detector module.

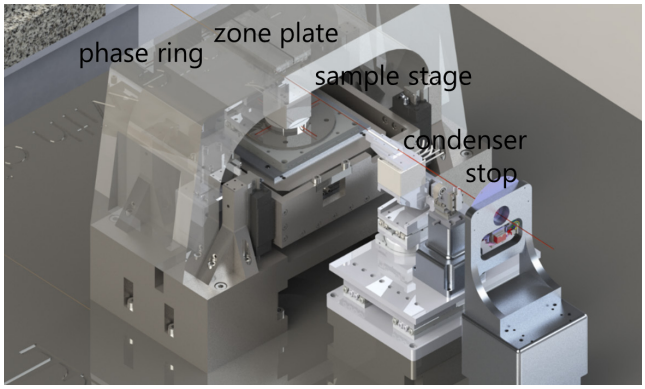

Fig. 4: Conceptual design of the TXM module.

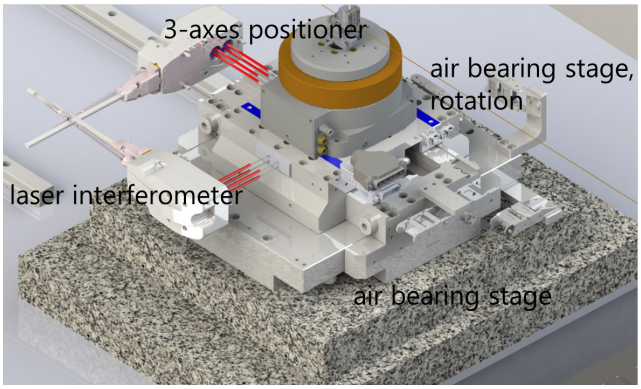

Fig. 5: The conceptually design of the PXM module.

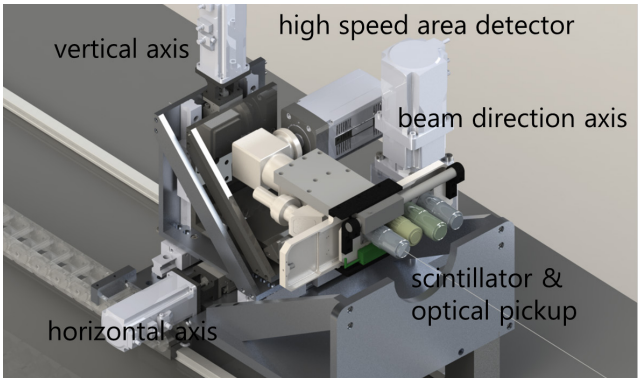

Fig. 6: Conceptual design of the detector module.

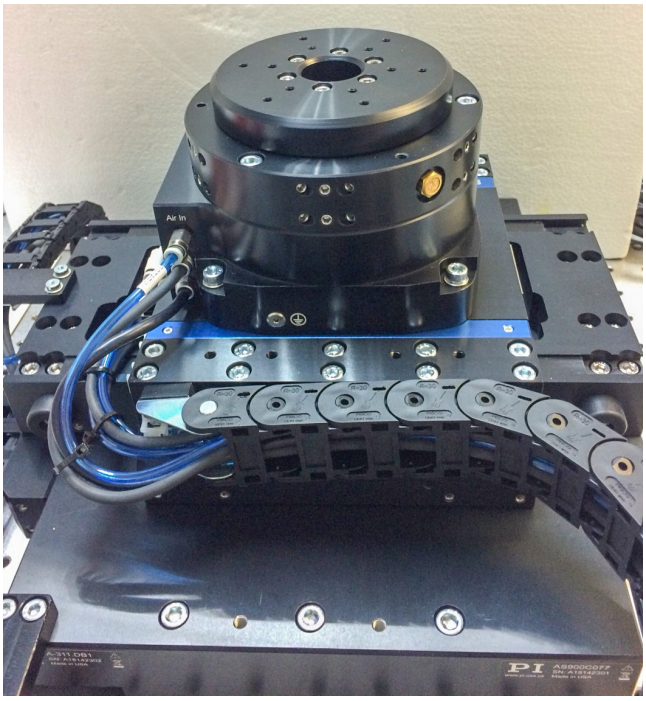

Fig. 7: Air bearing stage for PXM stage.

The limiting bottleneck of the schedule of this beamline is mainly the source – wiggler W100, which will be installed in TPS about the third quarter of 2020. The beamline will be completed then, but about two and half years from the present. For this reason, we continue to use the beamline of **SP8 12B2** to test new instruments and samples. The outlook of the stage is shown in **Fig. 7**.

In the past year, we have finished the report about the conceptual design (CDR) of the beamline, and sent it to members of the international committee for review. We have also finished the procurement of the key components of the PXM system, which was partially assembled and tested and which will be shipped to SPring-8 in the third quarter in 2018. (Reported by Gung-Chian Yin)

References

1. G.-C. Yin, Y.-F. Song, M.-T. Tang, F.-R. Chen, K.S. Liang, F.W. Duewer, M. Feser, W. Yun, and H.-P. D. Shieh, Appl. Phys. Lett. **89**, 221122 (2006).
2. G.-C. Yin, M.-T. Tang, Y.-F. Song, F.-R. Chen, K.S. Liang, F.W. Duewer, W. Yun, C.-H. Ko, and H.-P. D. Shieh, Appl. Phys. Lett. **88**, 241115 (2006).
3. Y.-T. Chen, T.-Y. Chen, J. Yi, Y.S. Chu, W.-K. Lee, C.-L. Wang, I. M. Kempson, Y. Hwu, V. Gajdosik, and G. Margaritondo, Opt. Lett. **36**, 1269 (2011).
4. R. Mokso, D. A. Schwyn, S. M. Walker, M. Doube, M. Wicklein, T. Müller, M. Stampanoni, G. K. Taylor, H. G. Krapp, Sci. Rep. **5**, 8727 (2015).
5. R. Mokso, C. M. Schleputz, G. Theidel, H. Billich, E. Schmid, T. Celcer, G. Mikuljan, L. Sala, F. Marone, N. Schlumpf, and M. Stampanoni, J. Synchrotron Rad. **24**, 1250 (2017).
6. Y. Wataru, N. Daiji, and K. Kentaro, Appl. Phys. Express, **10**, 052501 (2017).
7. T. Weitkamp, A. Diaz, C. David, F. Pfeiffer, M. Stampanoni, P. Cloetens, and E. Ziegler, Opt. Express **13**, 6296 (2005).
8. P. Cloetens, R. Barrett, J. Baruchel, J.-P. Guigay, and M. Schlenker J. Phys. D: Appl. Phys. 29, 133 (1996).
9. K. A. Nugent, T. E. Gureyev, D. F. Cookson, D. Paganin, and Z. Barnea, Phys. Rev. Lett. **77**, 2961 (1996).
10. A. V. Bronnikov, Opt. Commun.171, 239 (1999).
11. G. Schneider, Ultramicroscopy **75**, 85 (1998).
12. G.-C. Yin, F.-R. Chen, Y. Hwu, H.-P. D. Shieh, K. S. Liang, Appl. Phys. Lett. **90**, 181118 (2007).